# A Uranium(II) Arene Complex that acts as a Uranium(I) Synthon

Mark D. Straub,[a,b] Erik T. Ouellette,[a,b] Michael A. Boreen,[a,b] R. David Britt,[c] Khetpakorn Chakarawet,[c] Iskander Douair,[d] Colin A. Gould,[a] Laurent Maron,[d] Iker Del Rosal[d] David Villarreal,[c] Stefan G. Minasian,[b*] and John Arnold [a,b,*]

a. Department of Chemistry, University of California, Berkeley, CA, 94720, USA.

b. Chemical Sciences Division, Lawrence Berkeley National Laboratory, Berkeley, CA, 94720, USA

c. Department of Chemistry, University of California, Davis, Davis, CA, 95616, USA

d. Université de Toulouse et CNRS, INSA, UPS, UMR 5215, LPCNO 135 Avenue de Rangueil, 31077 Toulouse, France

** E-mail: arnold@berkeley.edu, sgminasian@lbl.gov*

*KEYWORDS: Uranium, arene, amidate, actinide*

**ABSTRACT:** Two-electron reduction of the amidate-supported U(III) mono(arene) complex U(TDA)$_3$ (**2**) with KC$_8$ yields the anionic bis(arene) complex [K[2.2.2]cryptand][U(TDA)$_2$] (**3**) (TDA = *N*-(2,6-di-*iso*-propylphenyl)pivalamido). EPR spectroscopy, magnetic susceptibility measurements, and calculations using DFT as well as multireference CASSCF methods all provide strong evidence that the electronic structure of **3** is best represented as a 5f$^4$ U(II) metal center bound to a monoreduced arene ligand. Reactivity studies show **3** reacts as a U(I) synthon by behaving as a two-electron reductant towards I$_2$ to form the dinuclear U(III)–U(III) triiodide species [K[2.2.2]cryptand][(UI(TDA)$_2$)$_2$(μ-I)] (**6**) and as a three-electron reductant toward cycloheptatriene

(CHT) to form the U(IV) complex [K[2.2.2]cryptand][U($\eta^7$-$C_7H_7$)$(TDA)_2$(THF)] (**7**). The reaction of **3** with cyclooctatetraene (COT) generates a mixture of the U(III) anion [K[2.2.2]cryptand][U$(TDA)_4$] (**1-crypt**) and U$(COT)_2$, while the addition of COT to complex **2** instead yields the dinuclear U(IV)–U(IV) inverse sandwich complex $[U(TDA)_3]_2$($\mu$-$\eta^8$:$\eta^3$-$C_8H_8$) (**8**). Two-electron reduction of the homoleptic Th(IV) amidate complex Th$(TDA)_4$ (**4**) with $KC_8$ gives the mono(arene) complex [K[2.2.2]cryptand][Th$(TDA)_3$(THF)] (**5**). The C–C bond lengths and torsion angles in the bound arene of **5** suggest a direduced arene bound to a Th(IV) metal center; this conclusion is supported by DFT calculations.

## INTRODUCTION

The seminal discovery of the first molecular uranium(II) complex [K[2.2.2]cryptand][U$(C_5H_4SiMe_3)_3$] in 2013[1] prompted a wave of new chemistry, including the syntheses of new U(II) complexes supported by cyclopentadienides,[2–5] amides,[5,6] and aryloxides.[7,8] These low-valent species have been the subject of intensive study due to their unusual multi-electron reactivity[9] and unconventional electronic structures: depending upon the supporting ligands and molecular symmetry of the complex, U(II) ions can have either a $5f^4$ or $5f^36d^1$ ground state electronic configuration, as determined by EPR spectroscopy, magnetic measurements, and DFT calculations.[10] Nonetheless, complexes of U(II) remain rare, and reactivity studies of isolable U(II) compounds are still sparse due to the unstable and highly reactive nature of these molecules.[3,9-11]

In certain recent cases, compounds with a formal oxidation state of U(III) or U(IV) have been found to undergo transformations analogous to those expected for U(II), prompting classification of these species as “U(II) synthons” or “masked U(II)”.[9] Similar strategies to achieve or mimic low valent reactivity have been employed in transition metal chemistry through the use of redox-active ligands; these complexes are often strongly reducing, facilitating a wide array of stoichiometric and catalytic transformations through electron transfer.[12,13] A common method for the stabilization of low-valent metal centers and “low-valent” synthons is via back-bonding into the π* system of an aromatic ligand, such as an arene.[12–14] Such complexes are often formed via reductive binding of aromatic solvent molecules,[15-17] though in some cases intramolecular reduction of a pendant aromatic group on the ligand is observed.[18,19] However, bound arenes can introduce a challenge in assigning the oxidation state of organometallic complexes due to the numerous ways in which these moieties can interact with metal centers. Arenes are often treated as redox-neutral when assigning formal oxidation states, leading to reported examples such as $[K[2.2.2]cryptand]_2[Zr(\eta^4\text{-}C_{10}H_8)_3]$ and $[Na[2.2.2]cryptand][Ta(\eta^4\text{-}C_{10}H_8)_3]$, which are described as Zr(–2) and Ta(–1), respectively.[20,21] When the arenes in these complexes are treated as direduced, however, the oxidation states of the metal centers would instead be Zr(IV) and Ta(V), thus occupying opposite ends of the spectrum of possible formal oxidation states for these metals.

With the exception of the U(II) tris(amide) $[K[2.2.2]cryptand][U(N(SiMe_3)_2)_3]$,[5] all previously reported examples of U(II) are supported either by cyclopentadienides or tethered arenes capable of engaging in δ-bonding interactions with uranium frontier orbitals.[22,23] In contrast to the Zr and Ta examples mentioned above, in which the arene ligands deviate significantly from planarity and display prominent distortions in bond angles and lengths upon binding,[24] δ-bonding interactions from U(II) can lead to more subtle arene distortions. This phenomenon is observed in both $U(NH(2,6\text{-}(2,4,6\text{-}^iPr_3C_6H_2)_2C_6H_3))_2$ and $[K[2.2.2]cryptand][((^{Ad,Me}ArO)_3Mes)U]$, each of which are described as U(II) with neutral arene ligands.[6,7] However, none of these previous examples of molecular U(II) contain a formally reduced arene ligand coordinated to the U(II) center, which may facilitate new modes of reactivity for U(II) complexes. Our goal was to introduce a versatile and hemilabile ligand system that could act as a σ-donor and δ-acceptor at discrete binding sites, thereby facilitating the stabilization of structurally related uranium complexes across multiple oxidation states and enabling us to probe their single- and multi-electron reactivity. To address these considerations, we turned to amidates, as this class of ligands is highly tunable, both sterically and electronically, and capable of adopting multiple binding modes.[25–29] By using an amidate ligand with an N-aryl substituent, the ligand is capable of binding to the metal center through the tethered arene moiety in addition to the more conventional O- and N-donor sites.[30] Through these efforts, we have isolated three new actinide arene complexes, including a U(II) bis(arene) complex containing a monoreduced arene ligand, and explored the reactivity and electronic structure of these unusual molecules.

## RESULTS AND DISCUSSION

### Synthesis of Uranium Arene Complexes

Drawing inspiration from our previous research on neutral U(IV) and anionic U(III) complexes supported by the *N*-(2,6-di-*iso*-propylphenyl)pivalamido (TDA) ligand,[25] we were interested in utilizing this ligand to access a neutral U(III) complex and other lower-valent species. As reported, reduction of the homoleptic, eight-coordinate U(IV) amidate $U(TDA)_4$ with $KC_8$ in the presence of 18-crown-6 gives the four-coordinate U(III) anion $[K(18\text{-crown-}6)][U(TDA)_4]$ (**1-crown**) (Scheme 3), with all four amidate ligands undergoing a change in coordination mode from κ$^2$-O,N to κ$^1$-O upon reduction of the metal center as evidenced in the solid-state by X-ray diffraction studies. We believed that lower-valent complexes could potentially be accessed by reduction of a neutral U(III) starting material, necessitating an alternative route to isolate a neutral, low-valent uranium complex using this ligand.[25]

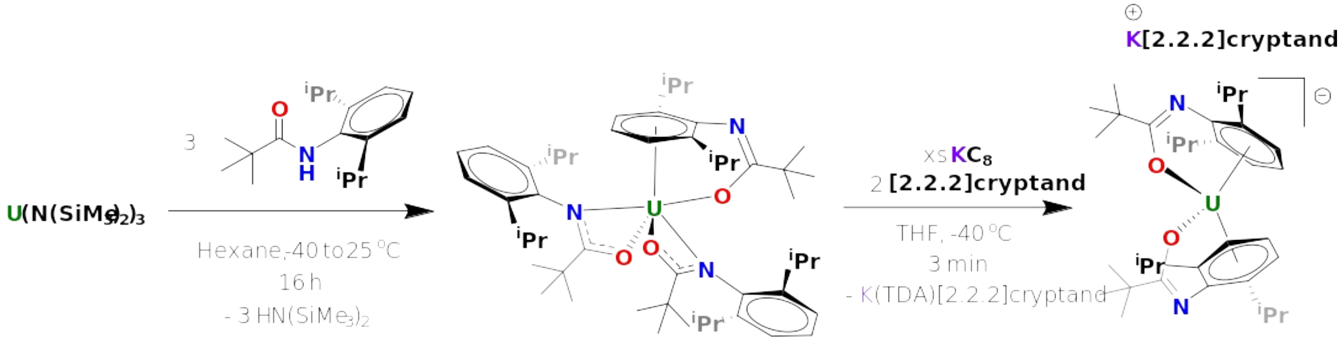

**2**
*68% yield*

**3**
*41% yield*

**Scheme 1.** Synthesis of the uranium mono(arene) complex U(TDA)$_3$ (**2**) and the uranium bis(arene) complex [K[2.2.2]cryptand][U(TDA)$_2$] (**3**) by two-electron reduction of **2**.

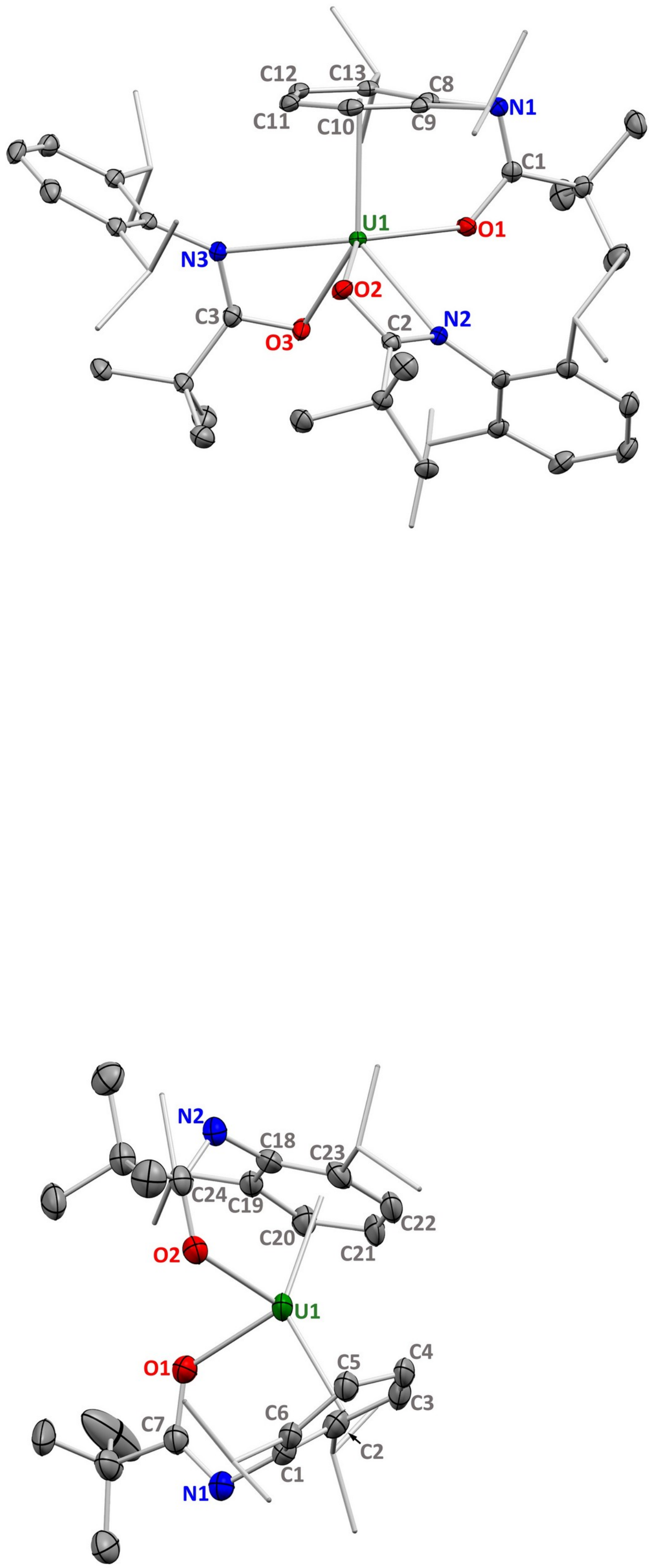

**Figure 1.** X-ray crystal structures of **2** (left) and **3** (right) with 50% probability ellipsoids. Hydrogen atoms and $[K[2.2.2]cryptand]^+$ are omitted, and *iso*-propyl groups are shown as capped sticks for clarity.

Accordingly, protonolysis of $U(N(SiMe_3)_2)_3$ by three equivalents of H(TDA) resulted in the formation of a dark purple product that was crystallized from pentane (Scheme 1). X-ray crystallography revealed this to be $U(TDA)_3$ (**2**), with two amidate ligands bound $\kappa^2$-O,N to the uranium center and one coordinated to uranium via the oxygen atom and an $\eta^6$-arene group (Figure 1). The bound arene in **2** is effectively planar, suggesting that aromaticity of the arene has not been lost upon binding to the uranium center;[14] this conclusion was further supported by experimental and computational studies (see below).

The six carbons of the bound arene in **2** adopt a planar geometry with U–C distances spanning the relatively narrow range of 2.899(2) to 2.988(2) Å and C–C bond lengths of 1.390(3) to 1.423(3) Å. The uranium–centroid distance of 2.602(2) Å is within the typical range for U(III) arenes.[31] Torsion angles for the bound arene, calculated by measuring the dihedral angle[19] formed by the C–C bonds on opposite sides of the arene, are relatively small – ranging from 2.5(2)° to 5.0(2)° – suggesting that no significant reduced character is present in this moiety. U–O and U–N distances of 2.310(2) to 2.347(2) Å and 2.581(2) to 2.652(2) Å, respectively, for the amidates in **2** are similar to corresponding distances for $\kappa^2$-O,N and $\kappa^1$-O amidates in $U(TDA)_4$ and **1-crown**.[25] Shorter M–O vs. M–N bond lengths are typical in amidate complexes of oxophilic metals such as actinides and early transition metals.[26,28,32,33]

Solid samples of complex **2** are stable indefinitely at room temperature under a nitrogen atmosphere. However, over the course of two months at room temperature a solution of **2** in $C_6D_6$ underwent near-complete disproportionation to $U(TDA)_4$ and a small quantity of additional unknown products. Addition of excess $KC_8$ and [2.2.2]cryptand to a THF solution of **2** at –40 °C resulted in a color change from dark purple to dark brown (Scheme 1). Dark brown crystals of this reduced product were grown from $Et_2O$, and X-ray crystallography revealed a new compound, $[K[2.2.2]cryptand][U(TDA)_2]$ (**3**) (Figure 1). In contrast to **2**, only two amidate ligands were attached to the metal center in **3**, and both arene groups were also bound to uranium in a manner reminiscent of a bent sandwich complex.

The crystal structure of **3** reveals that $[U(TDA)_2]^-$ possesses approximate $C_2$ symmetry in the solid-state; however, while both arenes are bound in an $\eta^6$ fashion to the uranium center, one of the arenes (comprised of carbon atoms C1–C6) is slightly distorted. C2 and C5 have U–C distances of 2.595(6) and 2.604(5) Å, respectively, whereas the remaining carbons in that arene are *ca.* 0.12 Å farther from U1 [2.689(6) to 2.745(6) Å]. Furthermore, the C1–C6 and C3–C4 bonds are slightly shortened relative to the remaining arene C–C bonds, which have torsion angles of 11.5(4) and 15.5(4)°; these metrics are within the typical range for a monoreduced arene ligand.[19] In contrast, the other bound arene (C18-C23) adopts a planar geometry, with U–C distances of 2.706(6) to 2.763(6) Å and C–C bond lengths of 1.389(7) to

1.440(6) Å. The torsion angles in this arene are minimal [0.9(4) to 4.6(4)°], suggesting that this ligand possesses no significant reduced character in the solid state.[19] U–centroid distances are 2.274(6) and 2.334(6) Å for the distorted and undistorted arenes, respectively; this contraction of *ca.* 0.3 Å from the U–centroid distance of **2** is consistent with increased U–arene back-bonding upon reduction (see below).[6] Similar U–centroid distances have been reported previously for the U(II) bis(amido) bis(arene) complex $U(NH(2,6\text{-}(2,4,6\text{-}^iPr_3C_6H_2)_2C_6H_3))_2$[6] and the U(II) mono(arene) complex [K[2.2.2]cryptand][((${}^{Ad,Me}$ArO)$_3$Mes)U].[7] As with **3**, both of these U(II) complexes also show substantial contraction of U–centroid distances upon reduction from U(III). The U–O bond lengths of 2.339(3) and 2.356(4) Å in **3** are longer than those in the $\kappa^1$-O amidates found on **1** and **2** and similar to the U–O bond lengths of the $\kappa^2$-O,N amidates bound to **2**.

The $^1$H NMR spectra of amidate complexes often show broad resonances due to ligand hemilability,[25-29] however the variable temperature $^1$H NMR spectra of **3** in $d_8$-THF (Figure S27) showed narrow linewidths over a wide temperature range (-89 to 27 °C). Resonances corresponding to each of the proton chemical environments were clearly identified – including the arene protons – despite the paramagnetic broadening which can obscure detection of ligands directly bound to the uranium center. In contrast to the inequivalent degree of distortion of the two arene ligands in the crystal structure of **3**, the $^1$H NMR spectrum of **3** in $d_8$-THF showed only one set of arene resonances, consistent with $C_2$ symmetry of the $[U(TDA)_2]^-$ anion in solution. This symmetry was maintained during variable temperature (VT) NMR experiments in the temperature range of –89 to 27 °C (Figure S27). These results suggest that in solution, any reduced character of the arene ligands appears to be delocalized across both arenes, a conclusion that is further corroborated by DFT calculations (see below).

Both the U(III) arene **2** and the Th(IV) arene **5** contain three amidate ligands, and each also has one amidate ligand that provides a pendant arene group that binds to the metal center. For **2**, the two ligands lacking a bound arene adopt a $\kappa^2$-O,N binding mode, while for **5** the two ligands lacking a bound arene adopt a $\kappa^1$-O binding mode. This rearrangement of all four amidate ligands from $\kappa^2$-O,N in **4** to $\kappa^1$-O in **5** could arise from steric congestion around the metal center upon binding the arene, though we believe it is more likely that increased electron density around the thorium center in **5** renders $\kappa^2$-O,N binding of the amidate ligand electronically unfavorable.[25,26,28] A similar change in ligand coordination geometry is observed upon reduction of the eight-coordinate uranium compound $U(TDA)_4$ to the four-coordinate anionic species **1-crown**[25] and **1-crypt**.

## Synthesis of a Thorium Arene Complex

As is common in studies of the early actinides, we sought structural, electronic, and reactivity comparison points to this unusual uranium chemistry through an investigation of the related thorium analogues. A small number of thorium complexes containing bound arenes have been reported,[34–36] but such species remain quite rare. The homoleptic thorium amidate complex Th(TDA)$_4$ (**4**) was synthesized via a salt metathesis reaction by stirring ThCl$_4$(DME)$_2$ with four equivalents of K(TDA) in THF (Scheme 2). Colorless crystals of **4** suitable for X-ray diffraction were grown from Et$_2$O. Complex **4** crystallizes as an eight-coordinate complex with all four amidate ligands bound κ$^2$-O,N to the metal center and an overall pseudo-$S_4$ symmetry (Figure 2), similar to the previously-reported uranium analog U(TDA)$_4$.[25] Th–O and Th–N bond lengths in **4** range from 2.343(3)–2.366(3) and 2.595(3)–2.724(3) Å, respectively. Although the Th–O bond lengths in **4** are similar to what we have previously reported for other homoleptic Th(IV) amidate complexes,[37] the Th–N bond lengths in **4** are longer by *ca.* 0.1 Å, likely due to the steric bulk of the TDA ligand.

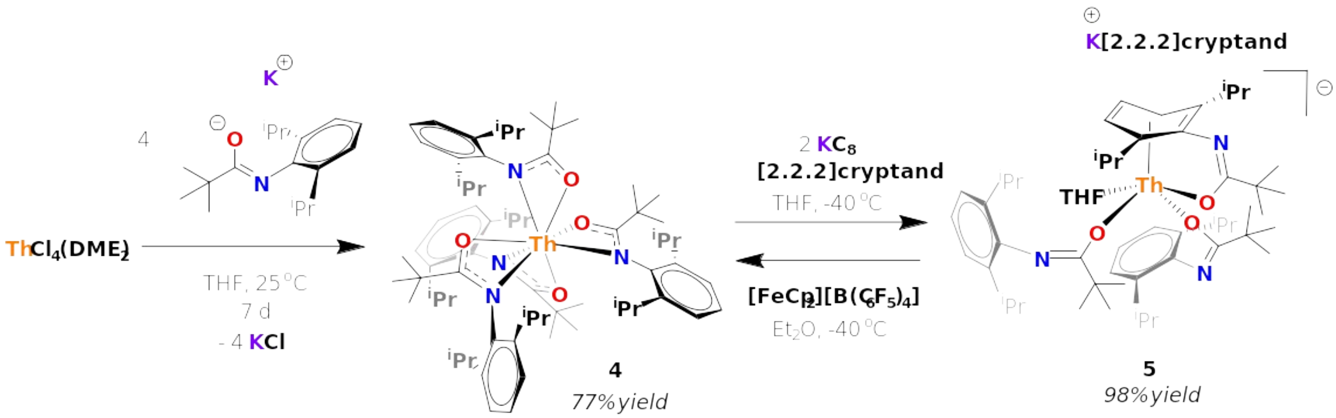

**Scheme 2.** Synthesis of Th(TDA)$_4$ (**4**) and the thorium mono(arene) complex [K[2.2.2]cryptand][Th(TDA)$_3$(THF)] (**5**) by two-electron reduction of **4**. Regeneration of **4** is achieved by oxidation of **5** with [FeCp$_2$][B(C$_6$F$_5$)$_4$].

To generate a thorium arene complex, two equivalents of KC$_8$ were added to a THF solution of **4** containing [2.2.2]cryptand at –40 °C, promptly causing a color change from colorless to orange (Scheme 2). X-ray diffraction of single crystals grown from Et$_2$O revealed this species to be the anionic complex [K[2.2.2]cryptand][Th(TDA)$_3$(THF)] (**5**), which contains a tethered η$^6$-arene ligand bound in a distorted geometry to the thorium center (Figure 2). The reduction of **4** did not proceed when Et$_2$O was used in place of THF; this may be due to the increased ease of electron transfer reactions in THF relative to the less polar $Et_2O$.[38] Weaker reducing agents, such as metallic sodium or $Cp^*_2Co$, were also unable to facilitate reduction of **4**.

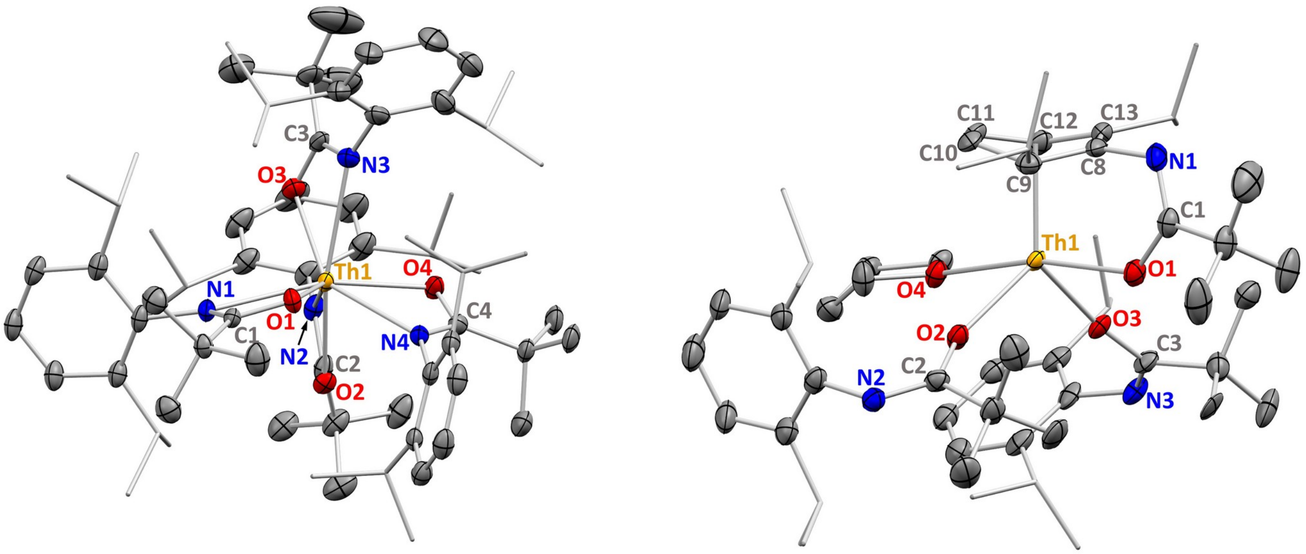

**Figure 2.** X-ray crystal structures of **4** (left) and **5** (right) with 50% probability ellipsoids. Hydrogen atoms and [K[2.2.2]cryptand]$^+$ are omitted, and *iso*-propyl groups are shown as capped sticks for clarity.

Structural examination of **5** shows that the bound arene moiety is bent significantly away from planarity, providing strong evidence that the ligand is reduced. For example, the variation of C–C bond lengths within the arene is reminiscent of a cyclohexadiene-like geometry: the C10–C11 and C13–C8 bonds have relatively short lengths of 1.358(9) and 1.374(9) Å, respectively, while the other four C–C arene bonds are significantly longer, ranging from 1.458(8)–1.513(9) Å. Torsion angles of 17.4(4) and 24.2(4)° also indicate reduction of the arene moiety; these values are consistent with a direduced arene bound to a Th(IV) center.[19,34] By comparison, all torsion angles in the C–C bonds of the two unbound arene moieties are at or below 2.0(5)°. The Th–C bond lengths range from 2.549(5) to 2.794(5) Å, with the carbon atoms C9 and C12 approximately 0.2 Å closer to the Th center than C8, C10, C11, and C13 due to the bent geometry of the bound arene.

### Reactivity of Actinide Arene Complexes

With the goal of investigating the single- and multi-electron reactivity of **2**, **3**, and **5**, we tested the behavior of these arene complexes towards a variety of small molecules and redox agents. The reaction of the U(III) monoarene **2** with one equivalent each of $KC_8$ and [2.2.2]cryptand at −40 °C in THF led to the formation of the anionic U(III) complex [K[2.2.2]cryptand][U(TDA)$_4$] (**1-crypt**) as the major product

(Scheme 3; Figure S1). The geometry and structural metrics of **1-crypt** are very similar to the previously-reported analogue **1-crown**,[25] with all four TDA ligands adopting a κ$^1$-O binding mode with U–O distances from 2.210(2) to 2.247(2) Å. It is interesting to note that two distinct anionic complexes, **3** and **1-crypt**, could be accessed from **2** simply by varying the stoichiometry of $KC_8$ and [2.2.2]cryptand. Ligand redistribution occurs in the formation of **3** and **1-crypt** from **2**: in the former case, one amidate ligand must be lost as the potassium salt; conversely, in the latter case, one amidate ligand must be gained. **1-crypt** was also synthesized via oxidation of **3** with one equivalent of $[Cp_2Fe][B(C_6F_5)_4]$ in $Et_2O$, with concomitant formation of $Cp_2Fe$ along with unidentified insoluble products (Scheme 3). Synthesizing an anionic U(III) species via oxidation is very unusual, indicating the highly reducing character of **3** and the tendency for ligand redistribution in this system; this is especially noteworthy given that the other synthetic pathways to **1** involve reduction of a starting material with $KC_8$.

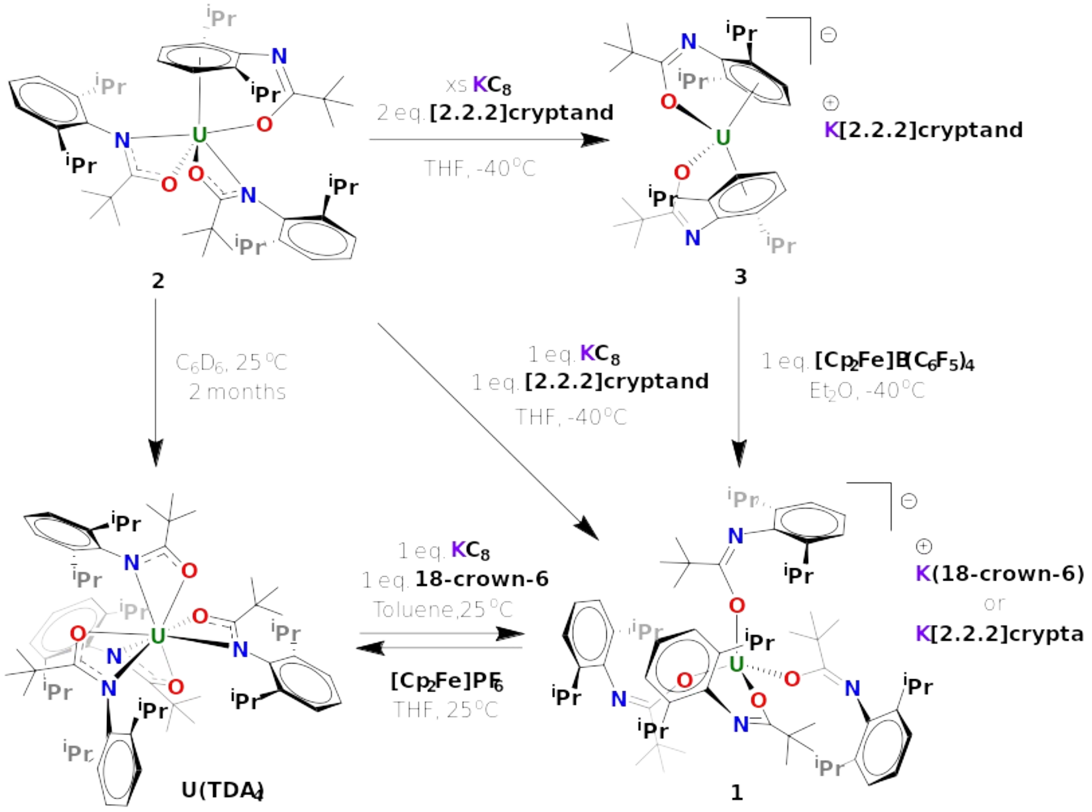

**Scheme 3.** Interconversion and redox reactivity of the uranium amidate complexes $U(TDA)_3$ (**2**), $[K[2.2.2]cryptand][U(TDA)_2]$ (**3**), $U(TDA)_4$, and $[KL][U(TDA)_4]$ (**1-crown**: L = 18-crown-6; **1-crypt**: L = [2.2.2]cryptand).

To determine if complex **3** could behave as a multi-electron reductant without the complication of ligand redistribution, we tested its reactivity towards elemental iodine. Addition of one equivalent of $I_2$ to a THF solution of **3** yielded the iodide-bridged U(III)–U(III) complex [K[2.2.2]cryptand][$(UI(TDA)_2)_2(\mu\text{-}I)$] (**6**), which was isolated as a blue solid from $Et_2O$ (Scheme 4; Figure 3). In this reaction, complex **3** can be considered as behaving as a U(I) synthon, with two-electron reduction of $I_2$ by each uranium center to yield a di-U(III) product in an overall four-electron reaction per molecule of **6**.

The solid state structure of **6** reveals a bridging iodide (I2) located 3.276(2) and 3.308(2) Å from U1 and U2, respectively, whereas the terminal iodide atoms I1 and I3 are found 3.068(2) and 3.081(2) Å from U1 and U2, respectively; these U–I bond lengths are consistent with other reported bridging and terminal U(III) iodides.[39] All four TDA ligands in **6** adopt $\kappa^2$-O,N binding modes, with two of those amidate oxygens (O2 and O3) also bridging the uranium centers, with bridging U–O distances of 2.440(6)–2.544(6) Å.

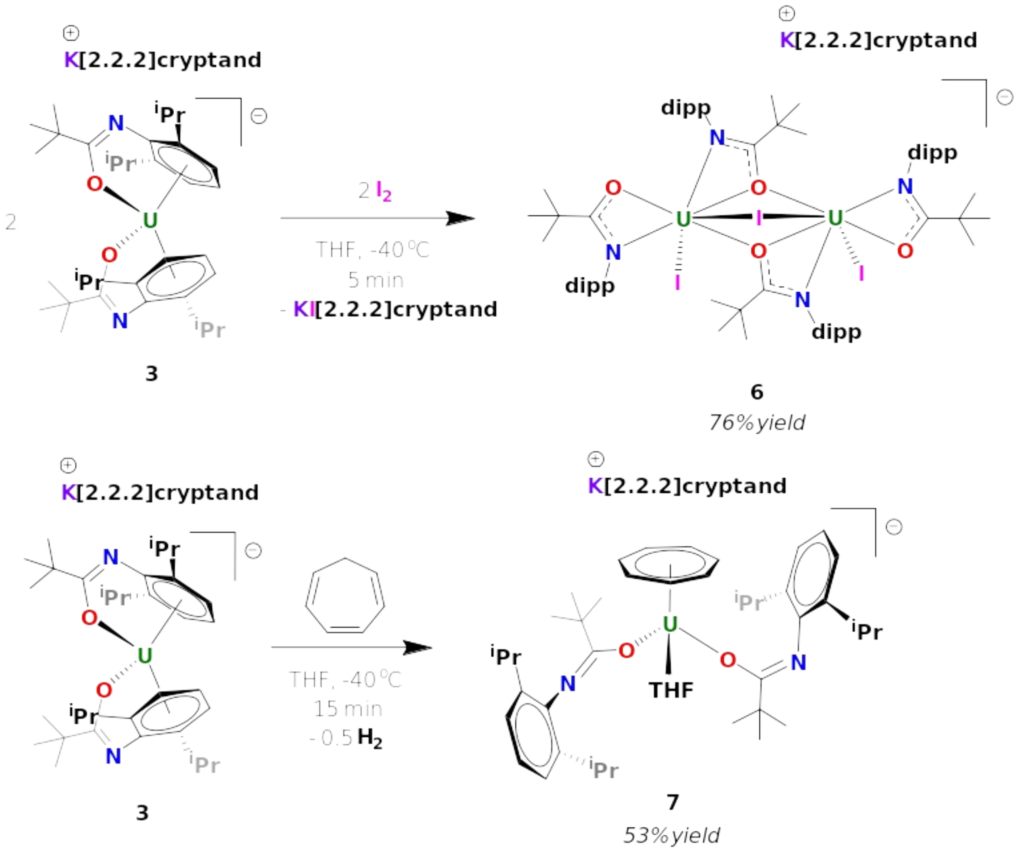

**Scheme 4.** Synthesis of the iodide-bridged U(III)–U(III) complex [K[2.2.2]cryptand][$(UI(TDA)_2)_2(\mu\text{-}I)$] (**6**) (top) and the U(IV) cycloheptatrienyl complex [K[2.2.2]cryptand][$U(\eta^7\text{-}C_7H_7)(TDA)_2(THF)$] (**7**) (bottom).

Following the isolation of **6**, we sought to further investigate the reactivity of **3** and discover whether this species would also behave as a U(I) synthon in other multi-electron transformations. Consequently, we turned to the [7]- and [8]-annulenes cycloheptatriene (CHT) and cyclooctatetraene (COT), respectively. These carbocycles can achieve aromaticity by three- and two-electron reduction, respectively, forming planar $C_7H_7^{3-}$ and $C_8H_8^{2-}$ anions. In contrast to the late transition metals, where the CHT moiety typically binds as the tropylium cation, $C_7H_7^+$, all examples of uranium CHT complexes contain this ligand in its trianionic form, $C_7H_7^{3-}$, a motif common for highly electropositive metals such as early transition metals, lanthanides, and actinides.[40-42] Given the substantial reducing power of **3**, we posited that a three-electron reduction of CHT should be feasible, leading to the formation of a U(IV) cycloheptatrienyl complex with concurrent loss of half an equivalent of $H_2$ from the ligand. Addition of CHT to a THF solution of **3** caused a color change in the solution from dark brown to maroon with concomitant formation of small gas bubbles, yielding a maroon product that was crystallized from $Et_2O$. Although small gas bubbles were observed during the synthesis of **7**, NMR confirmation of $H_2$ formation could not be obtained due to the presence of coincident $^1H$ NMR resonances from the [2.2.2] cryptand. The $^1H$ NMR spectrum of this compound indicated the presence of a new compound with a singlet at −47.90 ppm, in the expected region for a bound $C_7H_7^{3-}$ ligand.[43] X-ray crystallography confirmed this molecule to be [K[2.2.2]cryptand][U($\eta^7$-$C_7H_7$)(TDA)$_2$(THF)] (**7**), and DFT calculations support the assignment of **7** as containing a U(IV) center bound to a $C_7H_7^{3-}$ ligand (see below).

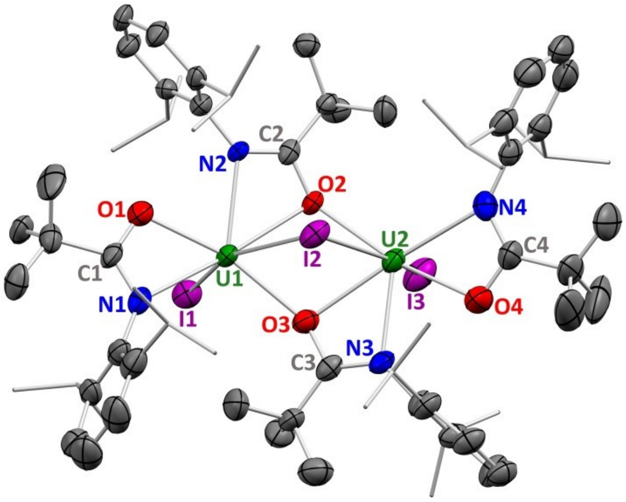

**Figure 3.** X-ray crystal structure of **6** with 50% probability ellipsoids. Hydrogen atoms and $[K[2.2.2]cryptand]^+$ are omitted, and *iso*-propyl groups are shown as capped sticks for clarity.

The three-electron oxidation from **3** to **7** provides another example of **3** reacting as a U(I) synthon (Scheme 4; Figure 4). Furthermore, three-electron reductions mediated by uranium complexes have been described only rarely.[22,44] To the best of our knowledge, complex **7** is the only reported example of a mononuclear uranium mono(cycloheptatrienyl) species. CHT complexes of uranium are quite rare: only two examples, the U(V) sandwich complex [K(18-crown-6)][$U(C_7H_7)_2$][45] and the U(IV)–U(IV) inverse sandwich complex [$U(BH_4)_2(THF)_5$][$(U(BH_4)_3)_2(\mu\text{-}\eta^7{:}\eta^7\text{-}C_7H_7)$][46] have been structurally characterized, and few other examples have been reported.[43] In contrast to the reactivity exhibited by **3**, the addition of CHT to **2** resulted in the formation of unstable products that decomposed quickly, regenerating some quantity of **2** among a mixture of other intractable products.

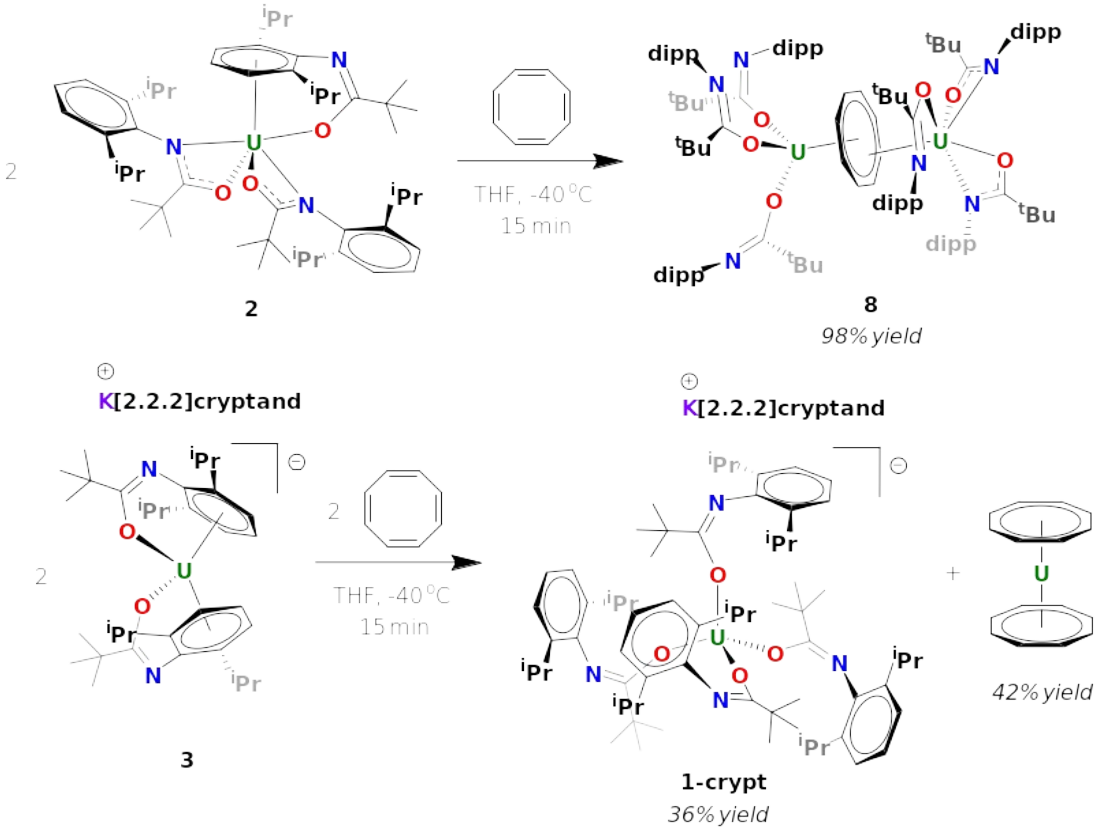

**Scheme 5.** Reactivity of $U(TDA)_3$ (**2**) and [K[2.2.2]cryptand][$U(TDA)_2$] (**3**) towards COT.

In comparison to the rarity of actinide CHT complexes, COT has been widely used as a ligand for the actinides,[47–51] and uranocene ($U(C_8H_8)_2$) has become one of the most studied organouranium complexes since it was first synthesized in 1968.[52] Following the isolation of **7**, we anticipated that **3** could potentially act as a two-electron reductant towards COT, generating a U(III) COT product. However, the addition of COT to a THF solution of **3** instead yielded the tetra-amidate anion **1-crypt** and uranocene as the two major products in 36% and 42% yield, respectively, indicative of oxidation at the metal and redistribution of the amidate ligands (Scheme 5). Similar reactivity has been documented for the U(II) complex [K(18-crown-6)][U($C_5H_4(SiMe_3)$)$_3$]; the addition of COT to this complex yielded a mixture of K(18-crown-6)][U($C_5H_4(SiMe_3)$)$_4$] and uranocene.[3] In contrast, addition of COT to a THF solution of **2** yielded a yellow product that was crystallized in high yield from pentane, which X-ray crystallography revealed to be the inverse sandwich complex [U(TDA)$_3$]$_2$(μ-$\eta^8$:$\eta^3$-$C_8H_8$) (**8**). Here, each uranium center reduces COT by one electron to give this U(IV)–U(IV) product; addition of excess COT to **8** did not result in any further reactivity.

The solid-state structure of **7** (Figure 4) shows a planar $C_7H_7$ ligand with U–C [2.563(4) to 2.577(4) Å] and C–C [1.382(6) to 1.431(7) Å] bond lengths exhibiting relatively narrow ranges, along with a U–$C_7H_7$ centroid distance of 1.991(4) Å; these are comparable to reported values for [K(18-crown-6)][U($C_7H_7$)$_2$].[45] The two amidates adopt a $\kappa^1$-O binding mode with U–O bond lengths of 2.255(2) and 2.272(2).

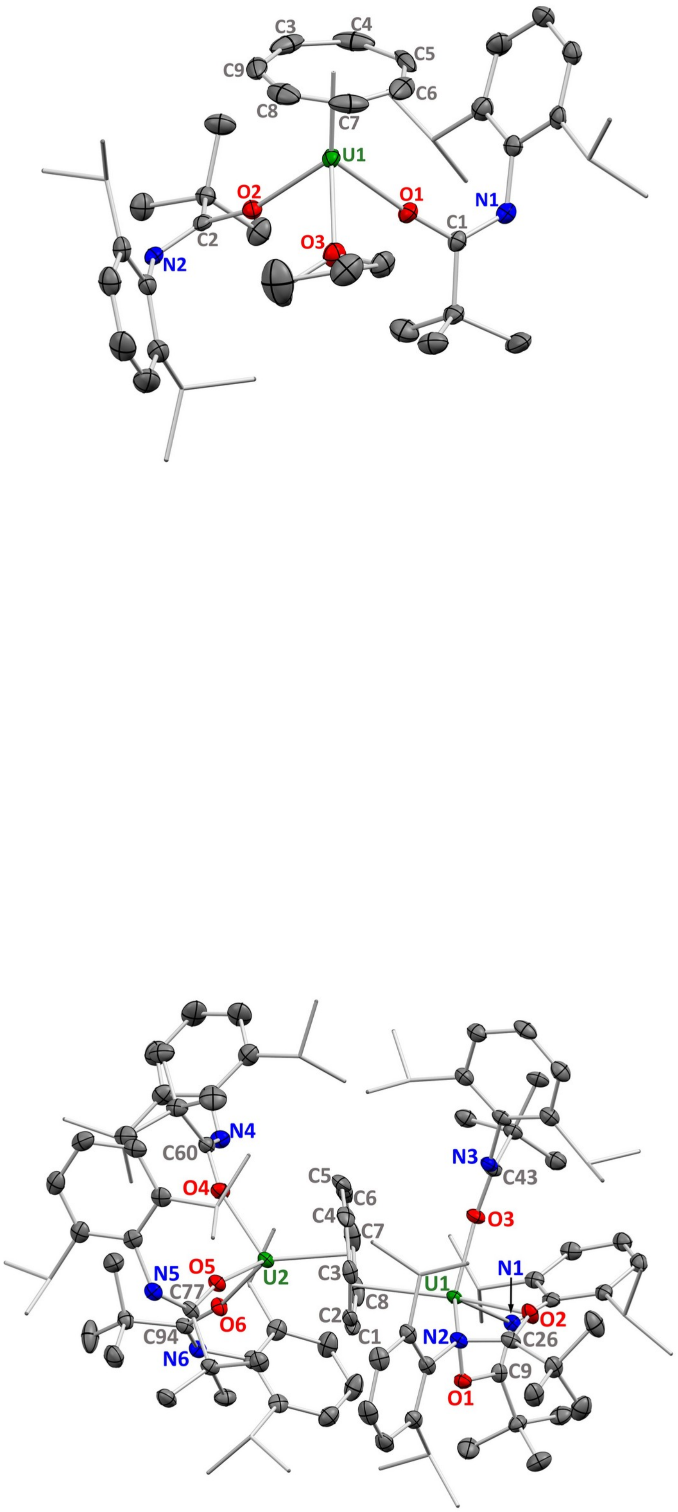

**Figure 4.** X-ray crystal structures of **7** (left) and **8** (right) with 50% probability ellipsoids. Hydrogen atoms and [K[2.2.2]cryptand]$^+$ are omitted, and *iso*-propyl groups are shown as capped sticks for clarity.

Complex **8** adopts an asymmetric inverse-sandwich geometry in the solid state with a planar $C_8H_8^{2-}$ fragment bridging the two uranium centers (Figure 4). The $C_8H_8^{2-}$ ligand is nearly planar, with C–C bond lengths ranging from 1.385(4) to 1.416(4) Å. The U2–C($C_8H_8$) distances range from 2.753(3) to 2.824(3) Å with a U2–centroid distance of 2.094(2) Å, consistent with an $\eta^8$ coordination mode for U2.[47] All three amidate ligands are bound $\kappa^1$-O to U2, with U2–O bond lengths ranging from 2.131(2) to 2.171(2) Å. In contrast, U1 appears to only be in contact with a portion of the $C_8H_8$ ring. Carbons C1–C3 are the only carbons found within 3 Å of the uranium center; the shortest contact is U1–C2: 2.708(3) Å, with the other end of the $C_8H_8$ ligand angled away from U1. These metrics suggest an $\eta^3$ coordination mode for U1, as has been previously described for the U(IV)–U(IV) $C_8H_8$ complex $[U(\eta^5\text{-}C_5Me_5)(\eta^8\text{-}C_8H_8)]_2(\mu\text{-}\eta^3\text{:}\eta^3\text{-}C_8H_8)$.[44] One of the amidate ligands is bound to U1 in a $\kappa^1$-O geometry [U1–O3: 2.105(2) Å], while the other two amidates adopt a $\kappa^2$-O,N binding mode [U1–O: 2.259(2) to 2.268(2) Å, U1–N: 2.480(2) to 2.488(2) Å].

Reactivity studies of the thorium arene **5** were limited by the highly reactive nature of this complex and by its thermal instability; we observed substantial decomposition of **5** in solution at –40 °C over a period of days. Attempts to study the reactivity of **5** towards most substrates capable of undergoing two-electron reduction led to intractable mixtures of products. However, the addition of one equivalent of $[Cp_2Fe][B(C_6F_5)_4]$ to **5** led to the regeneration of **4**, with concomitant formation of $Cp_2Fe$ and trace unidentified side products (Scheme 2).

## Electronic Structure of Uranium Arenes

### EPR Spectroscopy

EPR spectroscopy was performed to identify the electronic configuration of the ground state for complexes **2** and **3**. Continuous wave (CW) X-band EPR of a powdered sample of **2** shows a rhombic system with effective $g$-values of [3.605 1.264 0.626] giving a $g_{iso}$ = 2.24 (Figures 5 and S9). These $g$-values are consistent with other uranium(III) complexes previously reported with large orbital angular momentum.[53–55] The splitting in the EPR spectrum of **2** is too large to be accounted for by nuclear hyperfine interactions, and is likely the result of dipolar and/or exchange interactions between molecules in the solid state. Measurements on solution samples did not exhibit such splitting, suggesting that it is intermolecular in origin.

The EPR spectrum of **3** features a sharp, intense peak centered at 330 mT (Figures 5 and S10). This signal can be well simulated as an $S = {}^1/_2$ spin system with $g$ = [2.042 2.021 2.013]. This signal persists at temperatures as high as 40 K (Figure S11), indicating that the spin relaxation time is relatively long, which is characteristic of an organic radical. We attribute this signal to an arene ligand radical in **3**. The overall change in signal upon reduction of **2** to give **3** suggests that the uranium center is reduced to a non-magnetic ($5f^4$) ground state, with an EPR-silent integer spin, $S = 2$.[6-8] No other signals can be seen in **3** by EPR in the X-band, including an $S = {}^3/_2$ signal from a coupled metal-ligand system. Parallel-mode X-band CW-EPR of **3** was unable to reveal any integer spin signals that could be attributed to the uranium center, likely due to the low symmetry of **3** (Figure S10). The behavior of the U(II) ion in **3** (i.e. EPR non-active) is fully consistent with the discovery and characterization of the related U(II) arene complexes reported by Odom and coworkers[6] and by Meyer and coworkers.[7,8] The absence of transitions between spin states at 5 K indicates that the low-lying excited states are well separated, such that only a signal from the ligand radical is observed.

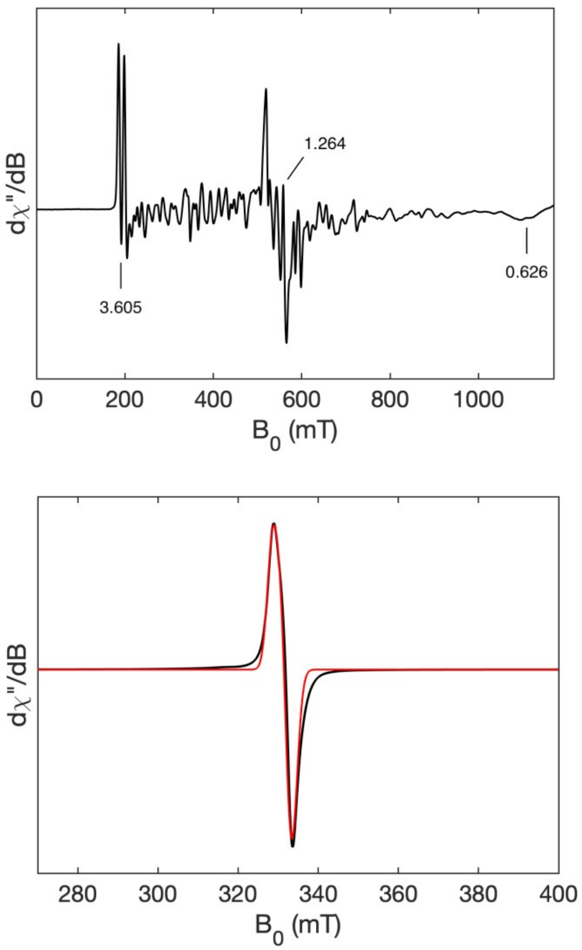

**Figure 5.** (Top) X-band (9.7 GHz) CW-EPR spectrum of a solid sample of **2** in perpendicular mode. The splitting seen in **2** is likely the result of dipolar and/or exchange interactions between molecules in the solid state. Conditions: temperature, 5K; microwave power, 0.2 mW; modulation amplitude 0.8 mT.

(Bottom) X-band (9.4 GHz) CW-EPR spectrum of a solid sample of **3** (black trace) in perpendicular mode. Simulated (red trace) with $S = 1/2$ spin system, $g$ = [2.042 2.021 2.013], and gStrain = [0.019

0.022 0.021]. Conditions: temperature = 5K; microwave power = 0.2 mW; modulation amplitude = 0.5 mT.

Complex **3** was additionally probed by high-field, high-frequency EPR at 130 GHz. An echo-detected field-sweep EPR spectrum of **3** measured at 4.5 K features an almost-axial signal arising from an $S = {}^{1}/_{2}$ spin that is well simulated by $g$ = [2.042 2.022 2.019] (Figure S12), in close agreement with $g$ parameters of the radical ligand extracted from the X-band spectrum. The deviation of the $g$ factor from the free-electron $g$ value ($g_e$ = 2.002) indicates anisotropy, confirming the proximity of the radical to the heavy uranium center bearing significant spin-orbit coupling.[56] No uranium-based signals were observed in echo-detected EPR at 4.5 K using 130 GHz irradiation, precluding further analysis of the electronic structure of **3**. Overall, EPR measurements indicate that the two-electron reduction of **2** by $KC_8$ results in a one-electron reduction of the metal center to give an integer spin $S$ = 2 uranium(II) center and a one-electron reduction of the ligand to give an $S = {}^{1}/_{2}$ arene radical, and that the U(II) atom and arene are decoupled in the ground state.

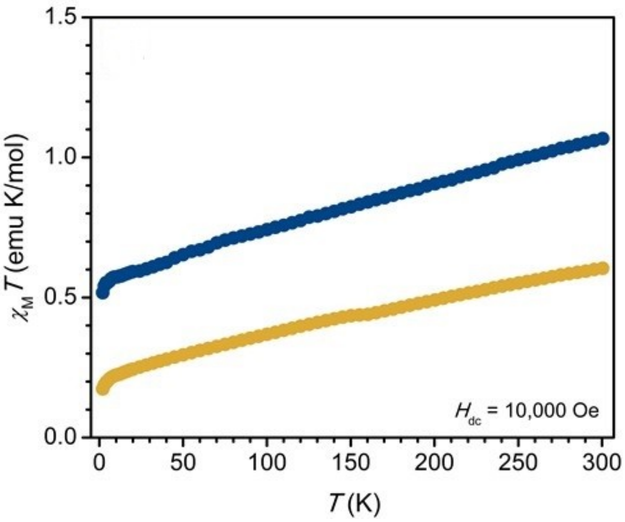

**Figure 6.** Dc magnetic susceptibility data for **2** (blue) and **3** (yellow) under an applied magnetic field of 10 kOe.

Magnetic Measurements

The electronic structure of **2** and **3** was further investigated by SQUID magnetometry. Variable-temperature dc magnetic susceptibility data for **2** and **3** were collected from 2 to 300 K under applied magnetic fields of 1, 10, and 70 kOe (Figures 6, S13, and S14). At 10 kOe, the $\chi_M T$ values for **2** are 1.07

emu K/mol at 300 K and 0.57 emu K/mol at zero K, which correspond to $\mu_{eff}$ values of 2.93 $\mu_B$ at 300 K and 2.13 $\mu_B$ for the ground state. These values are within the range reported for other uranium(III) complexes,[57] and also show good agreement with the value of 1.94 $\mu_B$ at zero K calculated using the *g* values obtained using EPR. By contrast, at 10 kOe **3** shows much smaller $\chi_M T$ values of 0.61 emu K/mol at 300 K and 0.23 emu K/mol at zero K, which correspond to $\mu_{eff}$ values of 2.20 $\mu_B$ at 300 K and 1.35 $\mu_B$ at zero K. The ground state $\mu_{eff}$ for **3** is somewhat lower than the value of 1.75 $\mu_B$ calculated using the EPR *g* values. However, both measurements show a trend towards decreasing magnetic susceptibility when moving from **2** to **3**,as expected if the U(II) center has a non-magnetic ground state. The $\chi_M T$ value for **3** shows a monotonic decrease with temperature, reaching a value of 0.17 emu K/mol at 2 K and 10 kOe. This low value can be attributed to the non-magnetic, singlet ground state anticipated for a $5f^4$ ion based on earlier studies of magnetic susceptibility in Pu(IV) compounds such as $(C_8H_8)_2Pu$ and $PuCl_6^{2-}$.[58,59] The smaller room temperature $\chi_M T$ value for **3** relative to **2** and the low $\chi_M T$ value at 2 K for **3** are also consistent with trends reported in previous studies of uranium(II) compounds.[3,4,6,7] In sum, these results corroborate EPR characterization of **2** and **3** and support the assignment of **3** as a uranium(II) compound with a monoreduced arene ligand.

## Electronic Structure Theory

The electronic structure of lanthanide and actinide arenes has been the subject of several earlier theoretical studies, particularly for high-symmetry molecules. [59-63] Here, density functional theory (DFT) calculations were performed on the uranium and thorium arenes to investigate their electronic structures, which all had low symmetry and appeared to be quite different based on our reactivity studies. We first considered the uranium complex **2** and the thorium anion in **5**, each of which possesses three TDA ligands with one coordinated arene. Figure 7 shows selected molecular orbitals calculated using DFT for both **2** and **5**. The ground state of **2** was found to be a quartet comprised of three occupied low-energy 5f orbitals that were entirely localized to the U center. Delta-bonding interactions between the uranium center and the arene are present in the HOMO–6, which is 2.36 eV lower in energy than the occupied $5f_{z^3}$ orbital (Figure S54). No significant degree of reduced character in the arene was found, and the unpaired spin density in **2** was calculated to be 3.00, consistent with the assignment as U(III). Complex **5** was optimized for both singlet and triplet spin states. The triplet state is comprised of a Th(III) center bound to a monoanionic arene and would be analogous to the bonding described above for **2**, while the singlet state is best represented as a Th(IV) center bound to a dianionic arene. Although the optimized geometries for both spin states were very similar, the singlet state was found to be 8.7 kcal/mol lower in energy, consistent with the assignment of complex **5** as Th(IV). Both spin states indicate the presence of δ-bonding interactions in the HOMO between the thorium center and the arene moiety. A bonding interaction between the thorium center and the arene is also seen in the HOMO–1, which contains two electrons in the π system of the arene for both the singlet and the triplet states (Figure S56). NBO analysis of the singlet state showed the Th–C bonds in **5** to be polarized towards carbon, with the bonding contribution from thorium arising mainly from 6d and 5f orbitals. To summarize, complex **2** has a U(III) oxidation state with three localized 5f electrons and a neutral arene, while complex **5** has a Th(IV) oxidation state and a doubly-reduced arene.

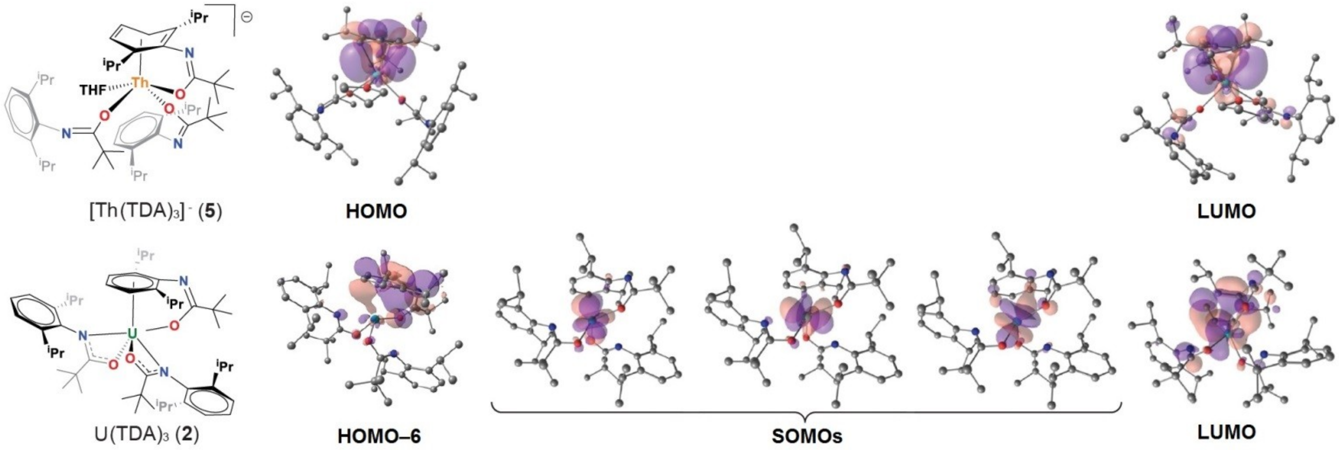

**Figure 7.** Selected molecular orbitals for the ground state of **2** (bottom) and **5** (top) calculated using DFT. For **2**, the ground state is a quartet, with three SOMO orbitals contain electrons primarily localized to nonbonding $5f_{z^3}$ (left), $5f_x(_{y^2–z^2})$ (center) and $5f_{y^3}$ (right) orbitals, while the HOMO–6 and LUMO orbitals display δ-bonding interactions between uranium $5f_{xyz}$ and arene π* orbitals. For **5**, the HOMO–1 is primarily of Th $6d_{z^2}$ character. The HOMO displays δ-bonding interactions between the Th $5f_{x(x^2-3y^2)}/6d_{(x^2-y^2)}$ orbitals and the arene π* orbitals, while the LUMO displays δ-bonding interactions between the Th $5f_{y(3x^2-y^2)}/6d_{xy}$ and the arene π* orbitals.

We also used DFT calculations to probe the electronic structure of the uranium arenes **3**, **7**, and **8**. Beginning with complexes **7** and **8**, the DFT calculations for both the [7]- and [8]-annulene complexes were unambiguous and consistent with formal U(IV) character (Figures S57 and S58). For example, the lowest-energy configuration for **7** was found to be a triplet state with U(IV) bound to a trianionic $[C_7H_7]^{3-}$

ligand and a uranium spin density of 2.29. The lowest-energy configuration for **8** was found to be a quintet spin state with two U(IV) ions bound to a dianionic $C_8H_8^{2-}$ ligand. The uranium centers had spin densities of 2.13 and 2.14, in line with a U(IV) oxidation state for each ion. The donation of the two uranium ions to the cyclooctatetraenyl ligand were significantly different, with values of 99.8 (σ) and 51.3 (π) kcal/mol for U1 vs. 241.9 (σ) and 118.4 (π) kcal/mol for U2; these substantial differences in energy are a result of $\eta^3$ versus $\eta^8$ binding of each uranium center to the bridging annulene ligand.

The DFT calculation for **3** showed that the U ion in **3** is best described by a U(III) oxidation state (electron configuration [Rn]7s(0.09)5f(3.03)6d(0.13)7p(0.03)). Closer inspection revealed three partially occupied 5f-orbitals and a doubly-reduced arene, which together housed four alpha spins and one beta spin that resulted in a ground state quartet (S = 3/2). Two of these SOMOs contain δ-bonding interactions between the $5f_{xyz}$ and $5f_x{}^3$ orbitals of the uranium, respectively, and the π* orbitals of both arene ligands, while the third SOMO is primarily of U $5f_z{}^3$ character. The LUMO of complex **3** contains an additional uranium-arene δ-bonding interaction between the $5f_{xyz}$ orbital of the uranium and the π* orbitals on one of the two arenes (Figure 8). The spin density of uranium in complex **3** was calculated to be 2.81, with some delocalization of spin density onto one of the two bound arenes. However, the U(III) ground state calculated with DFT contradicted the EPR measurement, which indicated that the U ion is EPR silent. Additionally, a sextet state for **3** was only 4.6 kcal/mol higher in energy; in this state, the U ion was calculated to have an unpaired spin density of 3.6, corresponding to a greater degree of reduction, and a uranium electron configuration of [Rn]7s(0.16)5f(3.50)6d(1.26)7p(0.29), suggesting formal U(I) character.

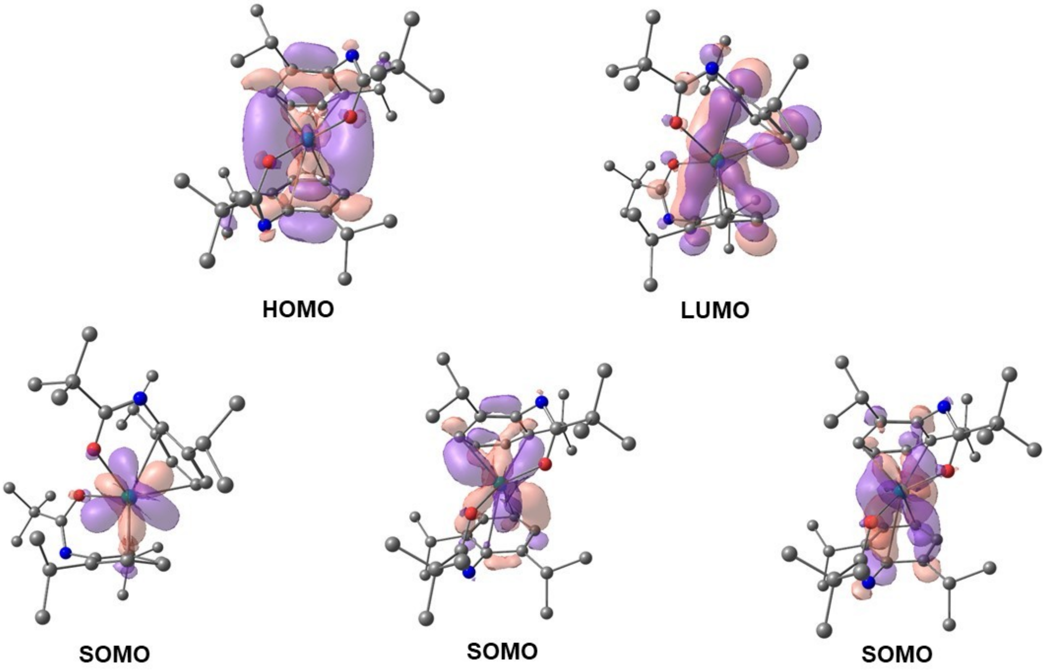

**Figure 8.** Selected molecular orbitals for the ground state of **3** calculated using DFT. One SOMO is primarily of U $5f_{z^3}$ character (left), while the other two SOMOs contain δ-bonding interactions between the $5f_{xyz}$ (center) and $5f_{x^3}$ (right) orbitals of the uranium and the π* orbitals of both arene ligands. The HOMO contains electrons primarily localized in the $5f_{x(x^2-3y^2)}$ and the orbital involved in the LUMO is primarily the $5f_{xyz}$.

The identification of the low energy states in the DFT calculation for **3** raised the possibility of a multiconfigurational ground-state. Hence, additional investigation of **3** was conducted using multireference methods (CASSCF),[64,65] which revealed a multiconfigurational ground state comprised of U(II) (69%) and U(III) (31%) character, with a pure U(II) state 4.6 kcal/mol higher in energy. Including spin-orbit coupling (SOC) resulted in a J = 4 ground state for **3** that is further split by the asymmetric ligand field into non-degenerate states, yielding a non-magnetic $M_J = 0$ ground state. Hence, although 3 might be viewed as a formal U(I) complex if the arenes are treated as formally neutral moieties,[6,12,19,24] the CASSCF calculations and experimental data provide convincing evidence against this view. This assignment is consistent with previous descriptions of electronic structure for $5f^4$ actinide systems[66] including $PuCl_6^{2-}$,[59] $(C_8H_8)_2Pu$,[58] $U(NH(2,6\text{-}(2,4,6\text{-}{}^iPr_3C_6H_2)_2C_6H_3))_2$,[6] and [K[2.2.2]cryptand][(($^{Ad,Me}$ArO)$_3$Mes)U].[7,8] Taken together with the experimental results described above, the calculations indicate that the electronic structure of **3** is best described as having a U(II) ion with a $5f^4$ electronic configuration, supported by a ligand framework with a monoreduced arene.

## CONCLUSIONS

We have synthesized an unusual uranium bis(amidate) complex with two tethered arene ligands (**3**) by two-electron reduction of the amidate-supported U(III) mono(arene) **2**. Complex **3** was characterized as U(II) with an overall monoreduced arene ligand framework based on evidence from EPR spectroscopy, SQUID magnetometry, and quantum chemical calculations. Complex **3** reacts as a U(I) synthon, behaving as a two- or three-electron reductant towards $I_2$ and cycloheptatriene, respectively, to give the U(III)–U(III) iodide complex **7** and the U(IV) cycloheptatrienyl complex **7**. In addition, we have synthesized an unusual example of a COT-bridged diuranium inverse sandwich complex (**8**) by addition of COT to the U(III) arene **2**, demonstrating the formation of uranium [6]-, [7]-, and [8]-annulene complexes supported by the same amidate ligand. For comparison, we also extended this work to thorium, preparing the anionic thorium tethered mono(arene) complex **5**, which contains a Th(IV) center coordinated to a direduced arene, by reduction of the homoleptic Th(IV) amidate complex **4**. Notably, many Th and U metallocenes adopt $6d^1$ electronic configurations upon reduction to Th(III) or U(II) oxidation states, instead of adding electrons to the 5f orbitals.[54,67-72] The $5f^4$ electronic configurations observed for **3** and related U(II) arene complexes,[6,7] combined with the formation of a direduced arene in **5** instead of a Th(III) complex, shows how ground state electronic configurations can be tuned by modifying the ligand environment.[73,74] Overall, the isolation of these new actinide arene complexes—along with their rich reactivity and diverse electronic structures—adds significantly to the burgeoning field of U(II) chemistry, and provides an interesting path forward to the chemistry of even more highly reduced uranium species.

## ASSOCIATED CONTENT

The Supporting Information is available free of charge on the ACS Publications website at DOI: 10.1021/acs.jacs.xxxxxx.

- Experimental details, crystallographic metrics, EPR and magnetism figures, computational details, NMR and IR spectra (DOC)
- Crystallographic data (CIF)

## AUTHOR INFORMATION

**Corresponding Authors**

John Arnold and Stefan Minasian

*arnold@berkeley.edu, sgminasian@lbl.gov*

**Author Contributions**

All authors have given approval to the final version of the manuscript.

## ACKNOWLEDGMENT

This work was supported by the Director, Office of Science, Office of Basic Energy Sciences, Division of Chemical Sciences, Geosciences, and Biosciences Heavy Element Chemistry Program of the U.S. Department of Energy (DOE) at LBNL under Contract No. DE-AC02-05CH11231. MDS was supported by a fellowship from the U.S. Department of Energy/National Nuclear Security Administration (DOE/NNSA) Nuclear Science and Security Consortium (NSSC) Graduate Student Program under Award Number(s) DE-NA0003180 and/or DE-NA0000979. Additional financial support was provided through NSF grants CHE-1800252 and CHE-2102603. We acknowledge the NIH (Grant S10-RR027172) for financial support of our X-ray crystallographic facility, and the Advanced Light Source, which is supported by the Director, Office of Science, Office of Basic Energy Sciences, of the U.S. Department of Energy under Contract No. DE-AC02-05CH11231. We thank the College of Chemistry's NMR facility for resources provided and the staff for their assistance; instruments are supported in part by NIH grant number S10OD024998. We are grateful to the reviewers for their helpful comments and suggestions.

## ABBREVIATIONS

TDA = *N*-(2,6-di-*iso*-propylphenyl)pivalamido
COT = cyclooctatetraene ($C_8H_8$)
CHT = cycloheptatriene ($C_7H_8$)

## REFERENCES

(1) MacDonald, M. R.; Fieser, M. E.; Bates, J. E.; Ziller, J. W.; Furche, F.; Evans, W. J. Identification of the +2 Oxidation State for Uranium in a Crystalline Molecular Complex, [K(2.2.2-Cryptand)][(C5H4SiMe 3)3U]. *J. Am. Chem. Soc.* **2013**, *135* (36), 13310–13313. https://doi.org/10.1021/ja406791t.

(2) Huh, D. N.; Ziller, J. W.; Evans, W. J. Chelate-Free Synthesis of the U(II) Complex, [(C5H3(SiMe3)2)3U]1-, Using Li and Cs Reductants and Comparative Studies of La(II) and Ce(II) Analogs. *Inorg. Chem.* **2018**, *57* (18), 11809–11814. https://doi.org/10.1021/acs.inorgchem.8b01966.

(3) Windorff, C. J.; MacDonald, M. R.; Meihaus, K. R.; Ziller, J. W.; Long, J. R.; Evans, W. J. Expanding the Chemistry of Molecular U2+ Complexes: Synthesis, Characterization, and Reactivity of the {[C5H3(SiMe3)2]3U}- Anion. *Chem. Eur. J.* **2016**, *22* (2), 772–782. https://doi.org/10.1002/chem.201503583.

(4) Guo, F. S.; Tsoureas, N.; Huang, G. Z.; Tong, M. L.; Mansikkamäki, A.; Layfield, R. A. Isolation of a Perfectly Linear Uranium(II) Metallocene. *Angew. Chem. Int. Ed.* **2020**, *59* (6), 2299–2303. https://doi.org/10.1002/anie.201912663.

(5) Ryan, A. J.; Angadol, M. A.; Ziller, J. W.; Evans, W. J. Isolation of U(Ii) Compounds Using Strong Donor Ligands, C5Me4H and N(SiMe3)2, Including a Three-Coordinate U(II) Complex. *Chem. Commun.* **2019**, *55* (16), 2325–2327. https://doi.org/10.1039/c8cc08767a.

(6) Billow, B. S.; Livesay, B. N.; Mokhtarzadeh, C. C.; McCracken, J.; Shores, M. P.; Boncella, J. M.; Odom, A. L. Synthesis and Characterization of a Neutral U(II) Arene Sandwich Complex. *J. Am. Chem. Soc.* **2018**, *140* (50), 17369–17373. https://doi.org/10.1021/jacs.8b10888.

(7) La Pierre, H. S.; Scheurer, A.; Heinemann, F. W.; Hieringer, W.; Meyer, K. Synthesis and Characterization of a Uranium(II) Monoarene Complex Supported by Δ backbonding. *Angew. Chem. Int. Ed.* **2014**, *53* (28), 7158–7162. https://doi.org/10.1002/anie.201402050.

(8) La Pierre, H. S.; Kameo, H.; Halter, D. P.; Heinemann, F. W.; Meyer, K. Coordination and Redox Isomerization in the Reduction of a Uranium(III) Monoarene Complex. *Angew. Chem. Int. Ed.* **2014**, *53* (28), 7154–7157. https://doi.org/10.1002/anie.201402048.

(9) Mazzanti, M.; Scopelliti, R.; Laurent, M.; Douair, I.; Palumbo, C.; Modder, D. Single Metal Four-Electron Reduction by U(II) and Masked "U(II)" Compounds. *Chem. Sci.* **2021**, *12*, 6153-6158. https://doi.org/10.1039/d1sc00668a.

(10) Moehring, S. A.; Evans, W. J. Evaluating Electron-Transfer Reactivity of Complexes of Actinides in +2 and +3 Oxidation States by Using EPR Spectroscopy. *Chem. Eur. J.* **2020**, *26* (7), 1530–1534. https://doi.org/10.1002/chem.201905581.

(11) MacDonald, M. R.; Fieser, M. E.; Bates, J. E.; Ziller, J. W.; Furche, F.; Evans, W. J. Identification of the +2 Oxidation State for Uranium in a Crystalline Molecular Complex, [K(2.2.2-Cryptand)][(C5H4SiMe 3)3U]. *J. Am. Chem. Soc.* **2013**, *135* (36), 13310–13313. https://doi.org/10.1021/ja406791t.

(12) Crabtree, R. H. Pi-Complexes. In *The Organometallic Chemistry of the Transition Metals*; John Wiley & Sons, 2014; pp 134–162. https://www.doi.org/10.1002/9781118788301.

(13) Norrby, P.-O. *Organotransition Metal Chemistry: From Bonding to Catalysis. John Hartwig*; 2010; Vol. 2. https://doi.org/10.1002/cctc.201000172.

(14) Muetterties, E. L.; Bleeke, J. R.; Wucherer, E. J.; Albright, T. A. Structural, Stereochemical, and Electronic Features of Arene-Metal Complexes. *Chem. Rev.* **1982**, *82* (5), 499–525. https://doi.org/10.1021/cr00051a002.

(15) Fostvedt, J. I.; Lohrey, T. D.; Bergman, R. G.; Arnold, J. Structural Diversity in Multinuclear Tantalum Polyhydrides Formed: Via Reductive Hydrogenolysis of Metal-Carbon Bonds. *Chem. Commun.* **2019**, *55* (88), 13263–13266. https://doi.org/10.1039/c9cc07686g.

(16) Diaconescu, P. L.; Arnold, P. L.; Baker, T. A.; Mindiola, D. J.; Cummins, C. C. Arene-Bridged Diuranium Complexes: Inverted Sandwiches Supported by δ Backbonding. *J. Am. Chem. Soc.* **2000**, *122*, 6108–6109. https://doi.org/10.1021/ja994484e.

(17) Arnold, P. L.; Halliday, C. J. V; Puig-Urrea, L.; Nichol, G. S. Instantaneous and Phosphine-Catalyzed Arene Binding and Reduction by U(III) Complexes. *Inorg. Chem.* **2021**, *60* (6), 4162-4170. https://doi.org/10.1021/acs.inorgchem.1c00327.

(18) Ziegler, J. A.; Lohrey, T. D.; Bergman, R. G.; Arnold, J. Hydroboration Reactivity of Niobium Bis(N-Heterocyclic Carbene)Borate Complexes. *Inorg. Chem.* **2018**, *57*, 5213–5224. https://doi.org/10.1021/acs.inorgchem.8b00247.

(19) Rosokha, S. V.; Kochi, J. K. Charge Transfer Effects on Arene Structure and Reactivity. In *Modern Arene Chemistry*; Astruc, D., Ed.; Wiley-VCH, 2002; pp 435–478. https://www.doi.org/10.1002/3527601767.ch13.

(20) Jang, M.; Ellis, J. E. Tris(η4-Naphthalene)Zirconate(2-). *Angew. Chem. Int. Ed.* **1994**, *33* (19), 1973–1975. https://doi.org/10.1002/anie.199419731.

(21) Brennessel, W. W.; Ellis, J. E.; Pomije, M. K.; Sussman, V. J.; Urnezius, E.; Young, V. G. Tris(η4-Naphthalene)- and Tris(1-4-η4-Anthracene)Tantalate(1-): First Homoleptic Arene Complexes of Anionic Tantalum. *J. Am. Chem. Soc.* **2002**, *124* (35), 10258–10259. https://doi.org/10.1021/ja020725y.

(22) Boreen, M. A.; Arnold, J. The Synthesis and Versatile Reducing Power of Low-Valent Uranium Complexes. *Dalton Trans.* **2020**, *49*, 15124–15138. https://doi.org/10.1039/d0dt03151h.

(23) Tian, J. N.; Zheng, M.; Li, L.; Schreckenbach, G.; Guo, Y. R.; Pan, Q. J. Theoretical Investigation of U(I) Arene Complexes: Is the Elusive Monovalent Oxidation State Accessible? *New J. Chem.* **2019**, *43* (3), 1469–1477. https://doi.org/10.1039/c8nj04722g.

(24) Ellis, J. E. Adventures with Substances Containing Metals in Negative Oxidation States. *Inorg. Chem.* **2006**, *45* (8), 3167–3186. https://doi.org/10.1021/ic052110i.

(25) Straub, M. D.; Hohloch, S.; Minasian, S. G.; Arnold, J. Homoleptic U(III) and U(IV) Amidate Complexes. *Dalton Trans.* **2018**, *47* (6), 1772–1776. https://doi.org/10.1039/C7DT04813K.

(26) Straub, M. D.; Leduc, J.; Frank, M.; Raauf, A.; Lohrey, T. D.; Minasian, S. G.; Mathur, S.; Arnold, J. Chemical Vapor Deposition of Phase-Pure Uranium Dioxide Thin Films from Uranium(IV) Amidate Precursors. *Angew. Chem. Int. Ed.* **2019**, *58* (17), 5749–5753. https://doi.org/10.1002/anie.201901924.

(27) Lee, A. V.; Schafer, L. L. Modular N,O-Chelating Ligands: Group-4 Amidate Complexes for Catalytic Hydroamination. *Eur. J. Inorg. Chem.* **2007**, *2007* (16), 2245–2255. https://doi.org/10.1002/ejic.200700036.

(28) Thomson, R. K.; Zahariev, F. E.; Zhang, Z.; Patrick, B. O.; Wang, Y. A.; Schafer, L. L. Structure, Bonding, and Reactivity of Ti and Zr Amidate Complexes: DFT and X-Ray Crystallographic Studies. *Inorg. Chem.* **2005**, *44* (24), 8680–8689. https://doi.org/10.1021/ic0502980.

(29) Drover, M. W.; Love, J. A.; Schafer, L. L. 1,3-N,O-Complexes of Late Transition Metals. Ligands with Flexible Bonding Modes and Reaction Profiles. *Chem. Soc. Rev.* **2017**, *46* (10), 2913–2940. https://doi.org/10.1039/C6CS00715E.

(30) Hagadorn, J. R.; Arnold, J. Tethered Bis-Amidinates as Supporting Ligands: A Concerted Elimination/σ-π Rearrangement Reaction Forming an Unusual Titanium Arene Complex. *Angew. Chem. Int. Ed.* **1998**, *37* (12), 1729–1731. https://doi.org/10.1002/(SICI)1521-3773(19980703)37:12<1729::AID-ANIE1729>3.0.CO;2-F.

(31) La Pierre, H. S.; Meyer, K. Activation of Small Molecules by Molecular Uranium Complexes. In *Progress in Inorganic Chemistry*; Barton, J., Ed.; Wiley, 2014; Vol. 58. https://doi.org/10.1002/9781118792797.ch05.

(32) Catherall, A. L.; Hill, M. S.; Johnson, A. L.; Kociok-Köhn, G.; Mahon, M. F. Homoleptic Zirconium Amidates: Single Source Precursors for the Aerosol-Assisted Chemical Vapour Deposition of ZrO2. *J. Mater. Chem. C* **2016**, *4* (45), 10731–10739. https://doi.org/10.1039/c6tc03631g.

(33) Huang, B.-H.; Yu, T.-L.; Huang, Y.-L.; Ko, B.-T.; Lin, C.-C. Reactions of Amides with Organoaluminum Compounds: Factors Affecting the Coordination Mode of Aluminum Amidates. *Inorg. Chem.* **2002**, *41* (11), 2987–2994. https://doi.org/10.1021/ic011072+.

(34) Korobkov, I.; Gambarotta, S.; Yap, G. P. A. The First Thorium Arene Complex: A Divalent Synthon. *Angew. Chem. Int. Ed.* **2003**, *42* (7), 814–818. https://doi.org/10.1002/anie.200390217.

(35) Korobkov, I.; Gambarotta, S. Cis Double Addition of CO2 to a Coordinated Arene of a Thorium Complex . *Organometallics* **2004**, *23* (23), 5379–5381. https://doi.org/10.1021/om049470i.

(36) Korobkov, I.; Vidjayacoumar, B.; Gorelsky, S. I.; Bilione, P.; Gambarotta, S. Attempting to Reduce the Irreducible: Preparation of a Rare Paramagnetic Thorium Species. *Organometallics* **2010**, *29* (3), 692–702. https://doi.org/10.1021/om900996n.

(37) Straub, M. D.; Ouellette, E. T.; Boreen, M. A.; Branson, J. A.; Ditter, A.; Kilcoyne, A. L. D.; Lohrey, T. D.; Marcus, M. A.; Paley, M.; Shuh, D. K.; Minasian, S. G.; Arnold, J. Thorium Amidates Function as Single-Source Molecular Precursors for Thorium Dioxide. *Chem. Commun.* **2021**, *57*, 4954-4957. https://doi.org/10.1039/d1cc00867f.

(38) Connelly, N. G.; Geiger, W. E. Chemical Redox Agents for Organometallic Chemistry. Chem. Rev. **1996**, *96* (2), 877-909. https://doi.org/10.1021/cr940053x.

(39) Baker, R. J. The Coordination and Organometallic Chemistry of UI3 and U{N(SiMe3)2}3: Synthetic Reagents Par Excellence. *Coord. Chem. Rev.* **2012**, *256* (23), 2843–2871. https://doi.org/10.1016/j.ccr.2012.09.011.

(40) Bennett, M. A. Metal Pi-Complexes Formed by Seven- and Eight-Membered Carbocyclic Compounds. In *Advances in Organometallic Chemistry*; Stone, F. G. A., West, R., Eds.; Elsevier, 1966; Vol. 4, pp 353–387. https://doi.org/10.1016/S0065-3055(08)60284-1.

(41) Jones, W. M.; Klosin, J. Transition-Metal Complexes of Arynes, Strained Cyclic Alkynes, and Strained Cyclic Cumulenes. In *Advances in Organometallic Chemistry*; Stone, F. G. A., West, R., Eds.; Academic Press, 1996; pp 147–217. https://www.doi.org/10.1002/CHIN.199830301.

(42) Tamm, M. Synthesis and Reactivity of Functionalized Cycloheptatrienyl – Cyclopentadienyl Sandwich Complexes. *Chem. Commun.* **2008**, 3089–3100. https://doi.org/10.1039/b802289e.

(43) Arliguie, T.; Lance, M.; Nierlich, M.; Ephritikhine, M. Inverse Cycloheptatrienyl Sandwich Complexes of Uranium and Neodymium. *Dalton Trans.* **1997**, No. 14, 2501–2504. https://www.doi.org/10.1039/A701352C.

(44) Evans, W. J.; Nyce, G. W.; Ziller, J. W. Formal Three-Electron Reduction by an f-Element Complex: Formation of of [{(C5Me5)(C8H8)U}2(C8H8)] from Cyclooctatetraene and [(C5Me5)3U]. *Angew. Chem. Int. Ed.* **2000**, *39* (1), 240–242.

(45) Arliguie, T.; Lance, M.; Nierlich, M.; Vigner, J.; Ephritikhine, M. Synthesis and Crystal Structure of [K(C12H24O6)][U(η-C7H7)2], the First Cycloheptatrienyl Sandwich Compound. *Chem. Commun.* **1995**, No. 2, 183–184. https://doi.org/10.1039/C39950000183.

(46) Arliguie, T.; Martine, L.; Vignerb, J.; Ephritikhinea, M.; Saclay, C. E. A. C. E.; Yvette, G. Inverse Cycloheptatrienyl Sandwich Complexes. Crystal Structure of [U(BH4)2(OC4H8)5[(BH4)3U(μ-η7,η7-C7H7)U(BH4)3]. *Chem. Commun.* **1994**, *179* (2), 847–848. https://www.doi.org/10.1039/C39940000847.

(47) Rausch, J.; Apostolidis, C.; Walter, O.; Lorenz, V.; Hrib, C. G.; Hilfert, L.; Kuehling, M.; Busse, S.; Edelmann, F. T. One Ligand Fits All: Lanthanide and Actinide Sandwich Complexes Comprising the 1,4-Bis(Trimethylsilyl)Cyclooctatetraenyl (=COT'') Ligand. *New J. Chem.* **2015**, *39*, 7656–7666. https://doi.org/10.1039/c5nj00991j.

(48) Diaconescu, P. L.; Cummins, C. C. Diuranium Inverted Sandwiches Involving Naphthalene and Cyclooctatetraene. *J. Am. Chem. Soc.* **2002**, *124*, 7660–7661. https://doi.org/10.1021/ja026200n.

(49) Liddle, S. T. Inverted Sandwich Arene Complexes of Uranium. *Coord. Chem. Rev.* **2015**, *293–294*, 211–227. https://doi.org/10.1016/j.ccr.2014.09.011.

(50) Grenthe, I.; Drożdżynński, J.; Fujino, T.; Buck, E. C.; Albrecht-Schmitt, T. E.; Wolf, S. F. Uranium. In *The Chemistry of the Actinide and Transactinide Elements*; Springer Netherlands: Dordrecht, pp 253–698, 2011. https://doi.org/10.1007/1-4020-3598-5_5.

(51) Cotton, S. *Lanthanide and Actinide Chemistry*; John Wiley & Sons, 2006. https://doi.org/10.1002/0470010088.

(52) Streitwieser, A.; Mueller-Westerhoff, U. Bis(Cyclooctatetraenyl)Uranium (Uranocene). A New Class of Sandwich Complexes That Utilize Atomic f Orbitals. *J. Am. Chem. Soc.* **1968**, *90* (26), 7364. https://doi.org/10.1021/ja01028a044.

(53) Formanuik, A.; Ariciu, A.-M.; Ortu, F.; Beekmeyer, R.; Kerridge, A.; Tuna, F.; Mcinnes, E. J. L.; Mills, D. P. Actinide Covalency Measured by Pulsed Electron Paramagnetic Resonance Spectroscopy. *Nat. Chem.* **2017**, *9*, 578–583. https://www.doi.org/10.1038/nchem.2692.

(54) Altman, A. B.; Brown, A. C.; Rao, G.; Lohrey, T. D.; Britt, R. D.; Maron, L.; Minasian, S. G.; Shuh, D. K.; Arnold, J. Chemical Structure and Bonding in a Thorium(Iii)-Aluminum Heterobimetallic Complex. *Chem. Sci.* **2018**, *9* (18), 4317–4324. https://doi.org/10.1039/c8sc01260a.

(55) Boreen, M. A.; Lohrey, T. D.; Rao, G.; Britt, R. D.; Maron, L.; Arnold, J. A Uranium Tri-Rhenium Triple Inverse Sandwich Compound. *J. Am. Chem. Soc.* **2019**, *141*, 5144–5148. https://doi.org/10.1021/jacs.9b01331.

(56) Kiernicki, J. J.; Cladis, D. P.; Fanwick, P. E.; Zeller, M.; Bart, S. C. Synthesis, Characterization, and Stoichiometric U–O Bond Scission in Uranyl Species Supported by Pyridine(Diimine) Ligand Radicals. *J. Am. Chem. Soc.* **2015**, *137* (34), 11115–11125. https://doi.org/10.1021/jacs.5b06217.

(57) Kindra, D. R.; Evans, W. J. Magnetic Susceptibility of Uranium Complexes. *Chem. Rev.* **2014**, *114* (18), 8865–8882. https://doi.org/10.1021/cr500242w.

(58) Karraker, D. G.; Stone, J. A.; Jones, E. R.; Edelstein, N. Bis(cyclooctatetrenyl)neptunium(IV) and bis(cyclooctatetrenyl)plutonium(IV). *J. Am. Chem. Soc.* **1970**, *92*, 4841-4845. https://doi.org/10.1021/ja00719a014.

(59) Karraker, D. G. Magnetic Susceptibilities of Tetravalent Plutonium Ion in Octahedral Compounds. *Inorg. Chem.* **1971**, *10*, 1564-1566. https://doi.org/10.1021/ic50102a002.

(60) Anderson, D. M.; Cloke, F. G. N.; Cox, P. A.; Edelstein, N.; Green, J. C.; Pang, T.; Sameh, A. A.; Shalimoff, G. On the Stability and Bonding In Bis(η-arene)Lanthanide Complexes. *Chem. Commun.* **1989**, 53-55. https://doi.org/ 10.1039/C39890000053.

(61) Arnold, P. L.; Petrukhina, M. A.; Bochenkov, V. E.; Shabatina, T. I.; Zagorskii, V. V.; Sergeev, G. B.; Cloke, F. G. N. Arene complexation of Sm, Eu, Tm and Yb atoms: a variable temperature spectroscopic investigation. *J. Organomet. Chem.* **2003**, *688*, 49-55. https://doi.org/ 10.1016/j.jorganchem.2003.08.028.

(62) Bochkarev, M. N. Synthesis, arrangement, and reactivity of arene-lanthanide compounds. *Chem. Rev.* **2002**, *102*, 2089-2117. https://doi.org/10.1021/cr010329i.

(63) Hong, G. Y.; Schautz, F.; Dolg, M. Ab initio study of metal-ring bonding in the bis($\eta^6$-benzene)lanthanide and -actinide complexes $M(C_6H_6)_2$ (M = La, Ce, Nd, Gd, Tb, Lu, Th, U). *J. Am. Chem. Soc.* **1999**, *121*, 1502-1512. https://doi.org/10.1021/ja9830400.

(64) Lukens, W. W.; Speldrich, M.; Yang, P.; Al., E. The Roles of 4f- and 5f-Orbitals in Bonding: A Magnetochemical, Crystal Field, Density Functional Theory, and Multi-Reference Wavefunction Study. *Dalton Trans.* **2016**, *45* (28), 11508–11521. https://doi.org/10.1039/C6DT00634E.

(65) Halbach, R. L.; Nocton, G.; Booth, C. H.; Maron, L.; Andersen, R. A. Cerium Tetrakis(Tropolonate) and Cerium Tetrakis(Acetylacetonate) Are Not Diamagnetic but Temperature-Independent Paramagnets. *Inorg. Chem.* **2018**, *57* (12), 7290–7298. https://doi.org/10.1021/acs.inorgchem.8b00928.

(66) Edelstein, N. M.; Lander, G. H. In *The Chemistry of the Actinide and Transactinide Elements*; 3rd ed.; Morss, L., Edelstein, N. M., Fuger, J., Eds.; Springer: Berlin, 2011; Vol. 4, p 2225-2306. https://doi.org/10.1007/1-4020-3598-5_5.

(67) Blake, P. C.; Lappert, M. F.; Atwood, J. L.; Atwood, J. L.; Zhang, H. M. The Synthesis And Characterization, Including X-Ray-Diffraction Study, Of $Th(\eta\text{-}C_5H_3(SiMe_3)_2)_3$ - The 1st Thorium(III) Crystal-Structure. *J. Chem. Soc. Chem. Commun.* **1986**, 1148-1149. https://doi.org/10.1039/C39860001148.

(68) Parry, J. S.; Cloke, F. G. N.; Goles, S. J.; Hursthouse, M. B. Synthesis and characterization of the first sandwich complex of trivalent thorium: A structural comparison with the uranium analogue. *J. Am. Chem. Soc.* **1999**, *121*, 6867-6871. https://doi.org/10.1021/ja9903633.

(69) Blake, P. C.; Edelstein, N. M.; Hitchcock, P. B.; Kot, W. K.; Lappert, M. F.; Shalimoff, G. V.; Tian, S. Synthesis, properties and structures of the tris(cyclopentadienyl)thorium(III) complexes $[Th\{\eta^5\text{-}C_5H_3(SiMe_2R)_2\text{-}1,3\}_3]$ (R = Me or ${}^t$Bu). *J. Organomet. Chem.* **2001**, *636*, 124-129. https://doi.org/10.1016/S0022-328X(01)00860-9.

(70) Langeslay, R. R.; Fieser, M. E.; Ziller, J. W.; Furche, F.; Evans, W. J. Synthesis, structure, and reactivity of crystalline molecular complexes of the $\{(C_5H_3(SiMe_3)_2)_3Th\}^{1-}$ anion containing thorium in the formal +2 oxidation state. *Chem. Sci.* **2015**, *6*, 517-521. https://doi.org/10.1039/C4SC03033H.

(71) Evans, W. J. Tutorial on the Role of Cyclopentadienyl Ligands in the Discovery of Molecular Complexes of the Rare-Earth and Actinide Metals in New Oxidation States. *Organometallics* **2016**, *35*, 3088-3100. https://doi.org/10.1021/acs.organomet.6b00466.

(72) Langeslay, R. R.; Chen, G. P.; Windorff, C. J.; Chan, A. K.; Ziller, J. W.; Furche, F.; Evans, W. J. Synthesis, Structure, and Reactivity of the Sterically Crowded $Th^{3+}$ Complex $(C_5Me_5)_3Th$ Including Formation of the Thorium Carbonyl, $[(C_5Me_5)_3Th(CO)][BPh_4]$. *J. Am. Chem. Soc.* **2017**, *139*, 3387-3398. https://doi.org/10.1021/jacs.6b10826.

(73) Wedal, J. C.; Furche, F.; Evans, W. J. Density Functional Theory Analysis of the Importance of Coordination Geometry for $5f^36d^1$ versus $5f^4$ Electron Configurations in U(II) Complexes. *Inorg. Chem.* **2021**, https://doi.org/10.1021/acs.inorgchem.1c02161.

(74) Gould, C. A.; Marbey, J.; Vieru, V.; Marchiori, D. A.; Britt, R. D.; Chibotaru, L. F.; Hill, S.; Long, J. R. Isolation of a Triplet Benzene Dianion. *Nat. Chem.* **2021**, *13*, 1001-1005. https://doi.org/10.1038/s41557-021-00737-8.

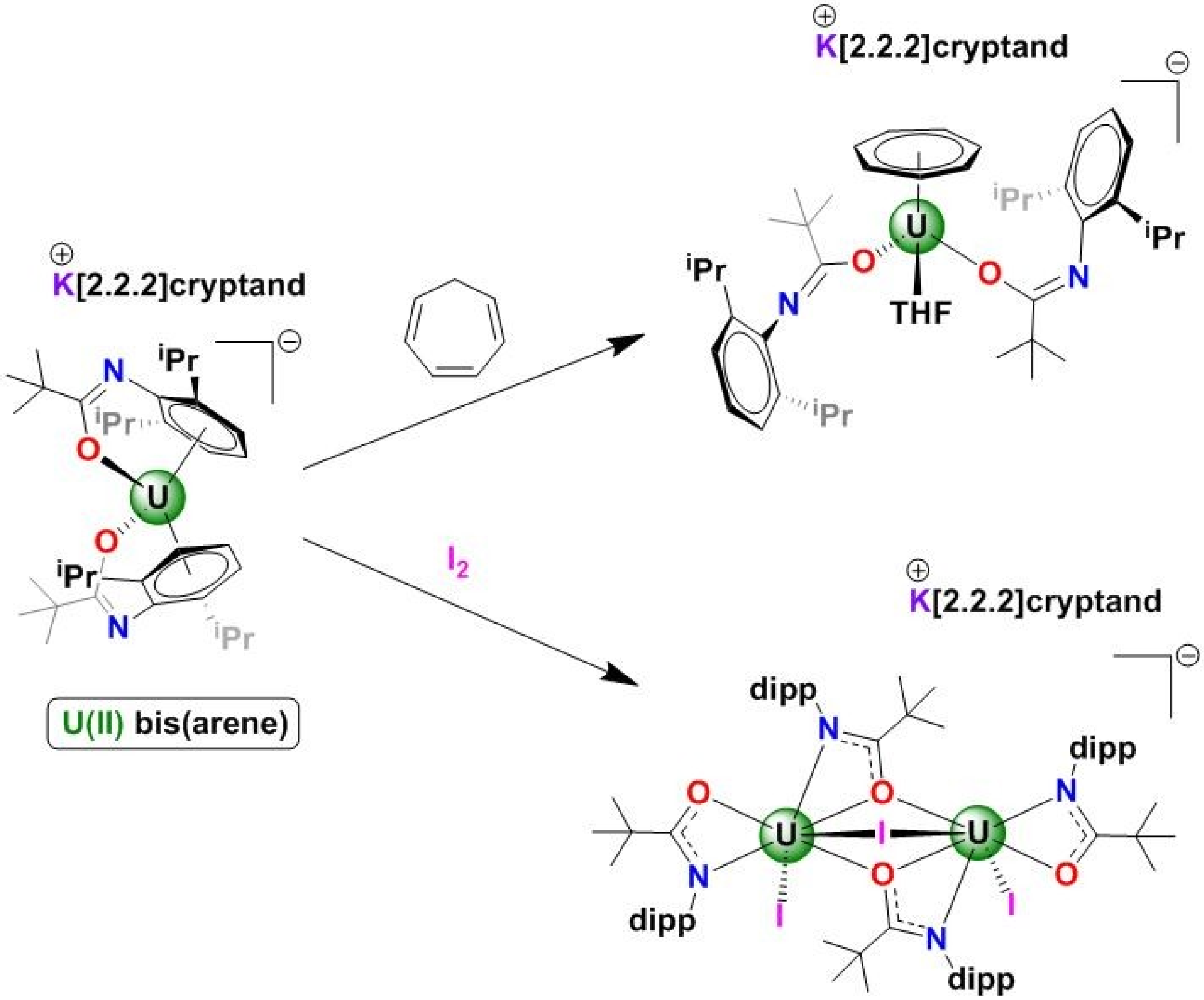

Uranium(II) bis(arene) reacts as a uranium(I) synthon